AIAA-2004-3852
Joint Propulsion Conference, Fort Lauderdale 2004

A Model for Design and Analysis of Regeneratively Cooled Rocket Engines

M.H. Naraghi*
Department of Mechanical Engineering, Manhattan College, Riverdale, NY 10471

S. Dunn† and D. Coats‡
SEA Inc., 1802 North Carson Street, Suite 200 Carson City, NV 89701

A new model for the design and analysis of a regeneratively cooled rocket engine is developed. In this model two proven rocket thermal analysis codes, TDK and RTE, were conjugated. The integration of these codes was accomplished via an interface file. The accuracy of this combined TDK-RTE model was examined by comparing its results to those of other methods for the SSME and experimental data for a liquid oxygen cooled RP1/LOX engine. Several of the additions and modifications incorporated into this model make it an excellent tool for designing the cooling circuits of regeneratively cooled engines.

I. Introduction

Design of innovative cooling methods for liquid rocket engines (LRE's) requires both a good physical insight on the workings of the engine and a method of calculating the effects of design changes on the heat transfer and cooling requirements of LRE's. There are several methods of calculating the effects of design changes ranging from simple correlations to full up Navier-Stokes solutions. Often coming up with a design requires several iterations. The Navier-Stokes solution, that takes a long time for a single run is not cost effective approach.

An innovative approach is developed for fast and accurate engineering calculation using the proven rocket engine codes, TDK[1] and RTE[2]. TDK is a code for rocket combustion gas chemistry and heat transfer, and RTE is for coolant flow convection and wall conduction. These codes are integrated together via an interface file. The TDK code computes the hot-gas-side heat transfer for a variety of wall temperatures and generates tables of Stanton number versus axial location and wall temperature. The RTE module then uses these tables to compute the wall and coolant flow thermal-flow characteristics. Depending on the cycle, the process can be iterated until convergence. The use of Stanton number and finite rate chemistry is critical to fast convergence of this model. The chemistry which occurs in the boundary layer has a significant effect on the recovery (adiabatic wall) enthalpy or temperature.

This combined TDK-RTE model is used to analyze two regeneratively cooled rocket engines. The first engine is the SSME (a LH2-LO2) and the second one is a RP1-LO2 engine with liquid oxygen as coolant. The results based on the present approach compared well with the published results for the SSME[3]. Also, the resulting wall temperature of the RP1-O2 engine at its throat shows an excellent agreement with the experimental data[4].

* Professor, mohammad.naraghi@manhattan.edu, Senior Member AIAA.
† Vice President, stu@seainc.com, Member AIAA.
‡ President, doug@seainc.com. Associate Fellow AIAA.

This combined TDK-RTE model can predict all needed thermal characteristics of regeneratively cooled engines, such as three-dimensional wall temperature distribution. An important design parameter in regeneratively cooled rocket engines is the coolant pressure at the exit of the cooling channels. This is due to the fact that the coolant, especially liquid hydrogen, is being used to run a turbo pump, and the pressure at the injector is known. The coolant pressure is influenced by the amount of heating from the hot-gas, as well as, the cooling channel geometry. The TDK-RTE model is capable accurately prediction the coolant pressure and temperature at various locations.

II. Procedure for Linking TDK and RTE

This new procedure for linking TDK and RTE is based on a lookup table of Stanton numbers that is generated by TDK. Figure 1 shows the hot gas-heat flux distribution at different axial locations for the SSME produced by running TDK at five different uniform wall temperatures (540, 750, 1000, 1250, 1500R). As shown in this figure there is about 16% difference between maximum and minimum wall heat fluxes at the throat. In order to speed up the convergence of RTE and improve the accuracy of the results, interpolations for evaluating the hot-gas-side heat fluxes are performed over a new variable based on the Stanton number,

$$\rho_e U_e St = \frac{\dot{q}_w}{h_{adb_w} - h_w}$$

As shown in Figure 2, using this new variable results in a much smaller variation with specified wall temperatures than with wall heat flux. To quantify the closeness of data using $\rho_e U_e St$ instead of wall heat flux, the relative differences of both variables for the maximum and minimum temperatures (1500 ºR and 740 ºR, respectively) are plotted in Figure 3. As shown in this figure, using $\rho_e U_e St$ reduces the relative difference by more than fourfold, in some instances to more than tenfold.

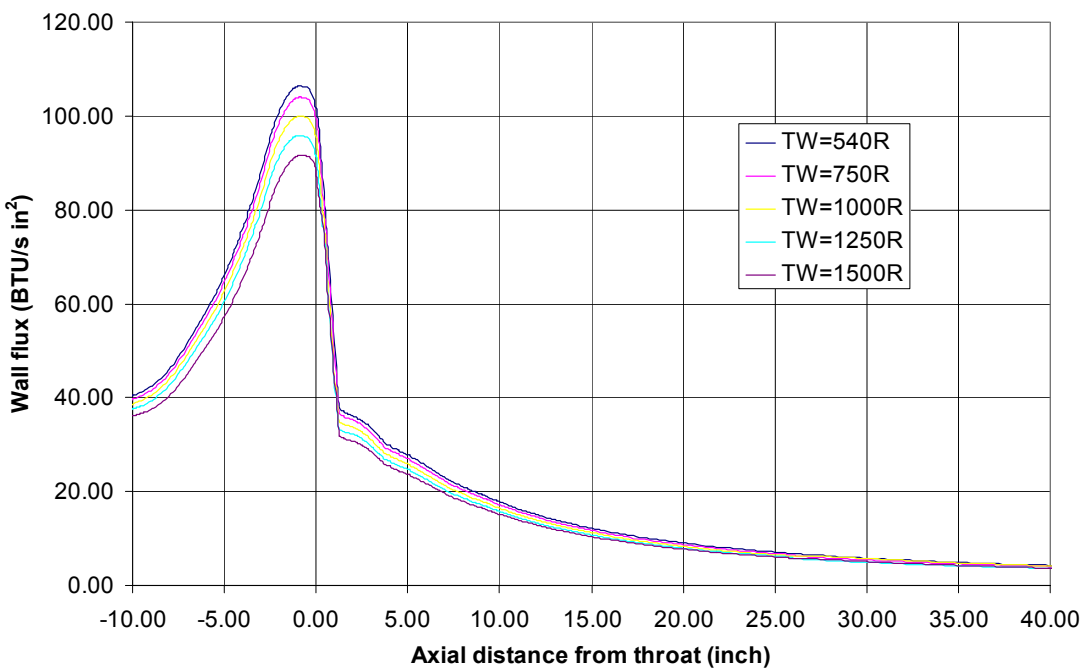

Figure 1. Wall Flux Distribution for SSME for Five Wall Temperature

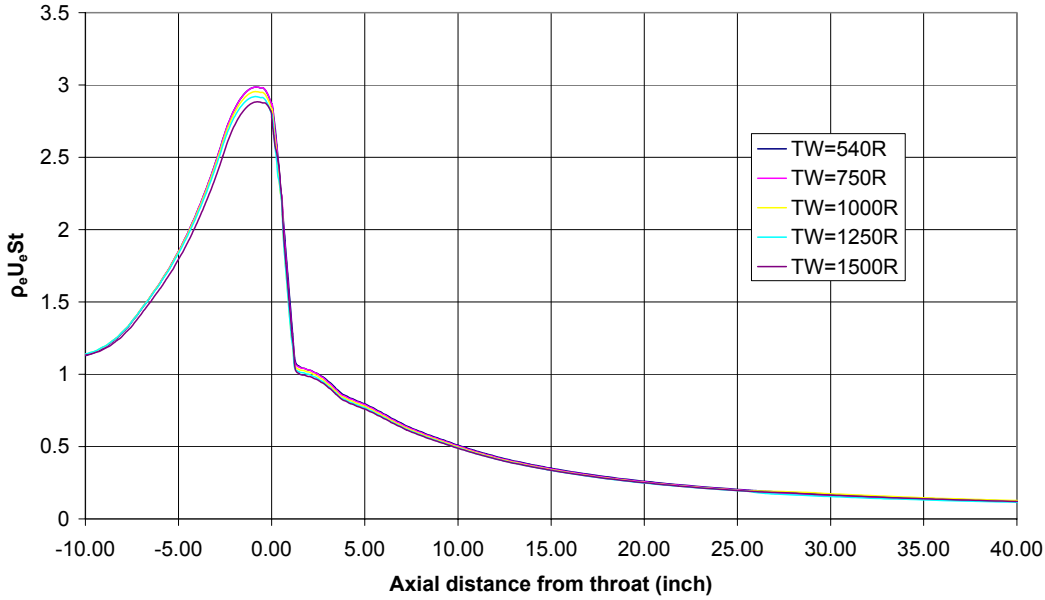

Figure 2. $\rho_e U_e St$ for the SSME at Different Wall Temperatures

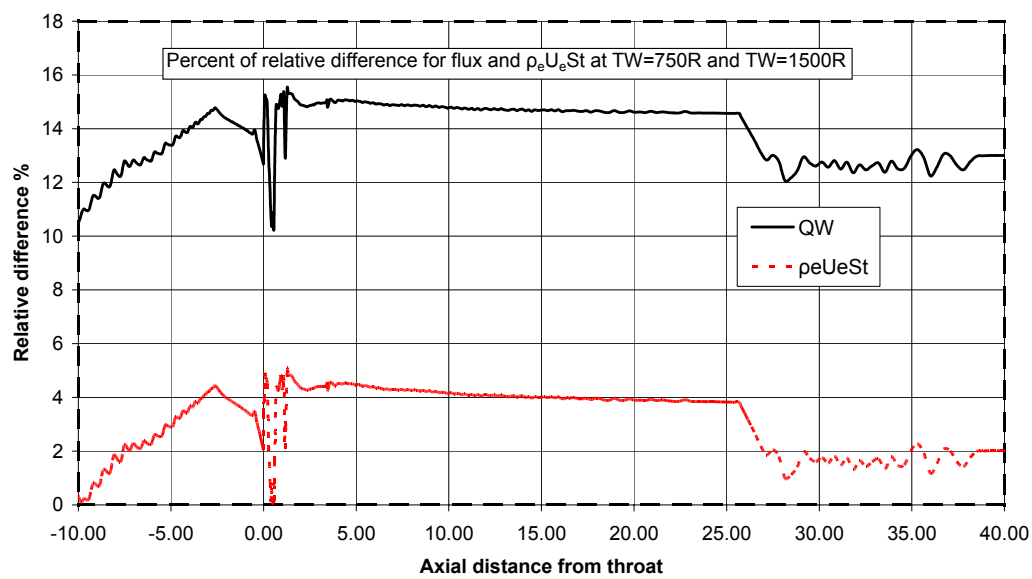

Figure 3. Percentage of Relative Difference of Wall Heat Flux and $\rho_e U_e St$ Between Maximum (1500R) and Minimum (540R) Wall Temperature for the SSME

This new model uses TDK for hot-gas-side heat flux calculations and generates a linkage file containing a table of wall heat fluxes, wall enthalpy, adiabatic wall enthalpy, and $\rho_e U_e St$ at several wall temperatures at various axial locations. Typically this table is produced for five uniform wall temperatures and it is generated by setting 'RTE=.TRUE.' in the TDK input file. The RTE module subsequently reads the TDK linkage file and interpolates with wall temperature and axial location to evaluate the local wall heat flux. Computational methodology used in RTE involves a number of iterations between hot-gas-side and coolant-side heat fluxes.

Flowchart of TDK-RTE interface is shown in Figure 4. TDK is executed with 'RTE=.TRUE.' in its NAMELIST input data. TDK, in addition to its standard output, produces a linkage file with a table of $\rho_e U_e St$ for a number of wall temperatures. Subsequently, running RTE, with 'OVERIDE=.TRUE.' in its input file, the resulting wall temperature distribution and coolant thermal characteristics are calculated using the TDK linkage table.

It should be noted that in a typical cooling circuit design process, TDK is run once and the linkage table of Stanton numbers do not change as long as the engine contour, chamber pressure and propellant characteristics remain the same. Refinements of cooling circuit, e.g. cooling channel dimensions and wall material can be done by re-running only RTE.

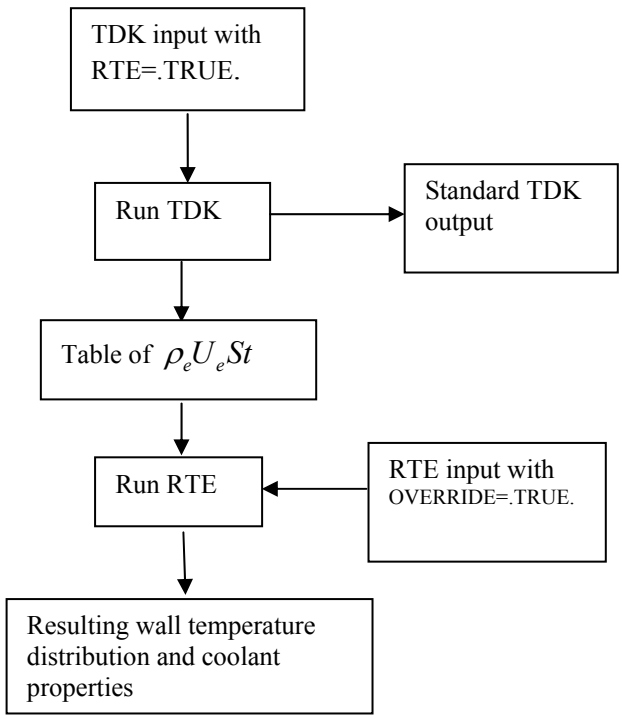

Figure 4. Flowchart of TDK-RTE Interaction

III. Example Calculations Testing Combinations of TDK and RTE

A. Analysis of the SSME

The Space Shuttle Main Engine (SSME) has been extensively analyzed by a number of investigators and much of the results are published in open literature. Therefore, to compare RTE predictions to published data, the combined TDK-RTE model was used to analyze the SSME.

Figure 5 shows a comparison of the computed SSME wall heat flux based on the present TDK-RTE model, a CFD model, and methods A and B reported by Wang et al.[3]. Method A and B results are based on the Rocketdyne and Pratt & Whitney models, respectively. The CFD's results are based on a NASA Marshall CFD model (see Wang et al.[3] for details of these models). These results show that the resulting wall heat flux based on the present approach, for the most part, is within the range of the published results. The maximum wall heat flux predicated by the present approach is in excellent agreement with that of the CFD model and method A (they are within 1% of each other). However, for axial location more than 10 inches

upstream of the throat, there is a large discrepancy between the heat flux based on the present approach and those published earlier. This discrepancy is due to the initialization of the boundary layer, which results in a spike in the wall heat flux. Method B under-predicts the maximum wall heat flux by about 15%. There is good agreement among all four models in the diverging section of the nozzle. It should be noted that between 5 and 10 inches upstream of the throat, the predictions of wall heat flux by the CFD model is about 25% higher than the other methods. This excessive heat flux would result in very high wall temperatures in a region where the coolant velocity is low and the temperature is relatively high. This issue will be discussed in detail when comparison is made between wall temperatures of the present approach and those of the CFD model.

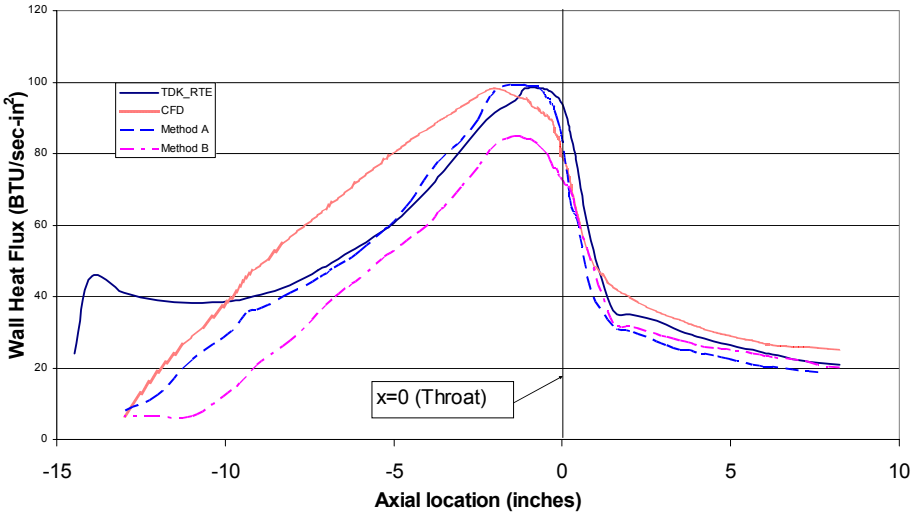

Figure 5. Comparison of SSME Wall Heat Flux Predicted by the TDK-RTE Model, a CFD Model and Methods A & B

A comparison of the SSME hot-gas-side wall temperature distributions for the present approach (TDK-RTE model) and the CFD method is shown in Figure 6. The resulting wall temperatures are highly dependent on the coolant flow characteristics, such as coolant channel aspect ratio and coolant properties. Additionally, the use of different coolant flow heat transfer correlations significantly affects the resulting predicted wall temperatures. The results of the TDK-RTE model presented in Figure 6 are based on two commonly used coolant heat transfer correlations, Dippery and Sabersky's (D & S) correlation[5] and Hendricks[6]. The CFD results are based on D & S's[5] correlation. The results of TDK_RTE based on the above coolant heat transfer correlations indicate that the wall temperatures are highly sensitive to the coolant heat transfer correlation.

The wall temperature at the throat (x=0) for the TDK-RTE model based on the Hendricks[6] correlation is about 20% higher than that of the CFD model. However, when the coolant correlation that is used by Wang et al. is implemented, the difference between temperatures becomes very small (about 3%). The wall temperatures based on the CFD model are generally lower than TDK-RTE model at the diverging section of the nozzle. However, the temperatures become considerably higher (more than 20% for D & S correlation and 15% for Hendricks correlation) for both the chamber and converging sections of the nozzle. Results of the CFD model indicates a very large axial temperature gradient at the throat (a temperature change of about 600 $^{\circ}$R in one-inch). The CFD model predicts a maximum wall temperature that is 20 $^{\circ}$R less than the NAROY-Z (copper alloy used in SSME) allowable temperature.

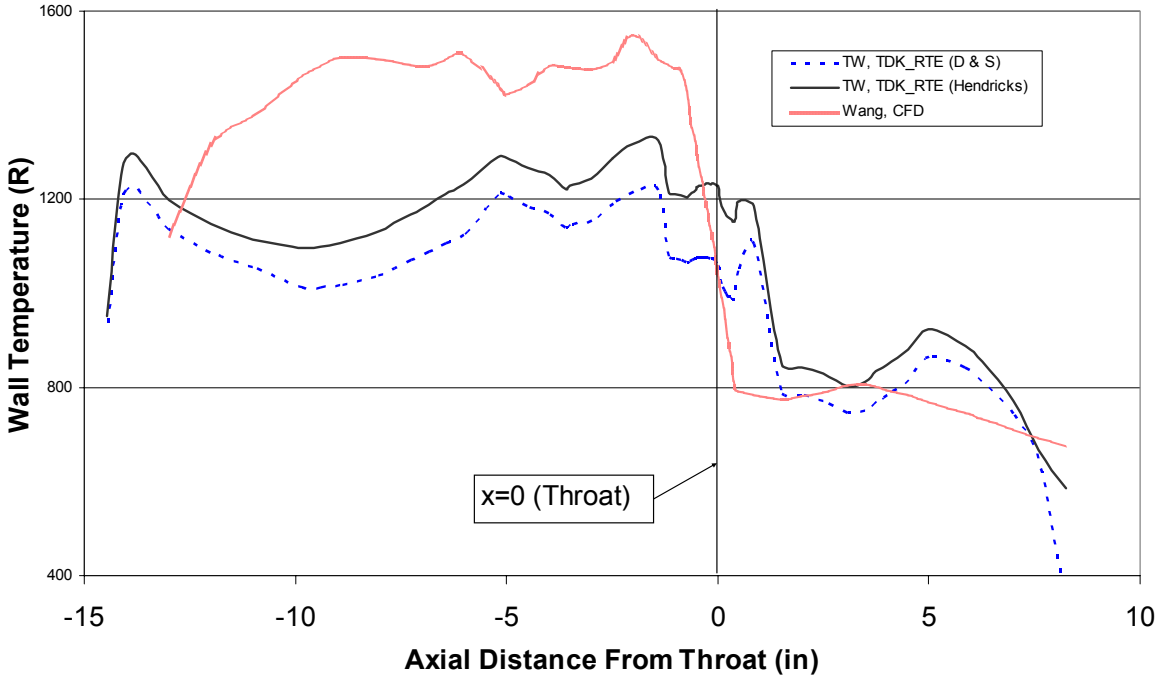

Figure 6. Comparison of SSME Hot-gas-side Wall Temperatures Predicated by the TDK-RTE Model (Dipprey-Sabersky's and Hendricks' correlations) and a CFD Model (Wang et al.)

It is not unusual to have higher wall temperature at the chamber and converging section of the nozzle than that of the throat area. This higher temperature can be due to several factors:

1. The maximum wall heat flux is upstream of the throat (see Figure 5).
2. Cooling channels are widening as coolant travels from throat toward chamber, which results in slower coolant velocity and lower heat transfer coefficient.
3. Higher coolant temperature upstream of the throat.
4. Higher gas temperature upstream of the throat.

The postprocessor for the new version of RTE is based on TecPlot®, which is capable of producing three-dimensional plots of the wall temperature distribution along the cooling channel. The user can view the temperature distributions at selected stations or zoom into an area of interest (e.g., the throat area). Figure 7 shows a three-dimensional temperature distribution along a cooling channel for the SSME. Due to the long and narrow cooling channels configuration, it is impossible to see the temperature distribution for every station in one frame. However, a user can view an enlarged temperature distribution at selected stations. The user can also focus on any specific axial location along the cooling channel, and examine the temperature distributions in detail, as shown in Figure 8 (throat area of the SSME). The three-dimensional graphic output enables a user to examine temperature distribution and gradient. For example, the temperature distribution shown in Figure 7 indicates that there is a large radial temperature gradient three inches upstream of the throat (at axial location z=-3 inch). Also, a user might be interested in knowing the wall temperature at the surface of the cooling channel, especially when the coolant is a hydrocarbon fuel (excessive coolant wall temperature would result in coking). Without three-dimensional temperature distributions, the user would be required to go over pages of temperature distribution output to deduce the required temperatures or temperature distributions (61 pages of temperature distribution for the SSME engine studied here). Additionally, the three-dimensional temperature distribution reveals all dimensional

details of the cooling channels. If there are any dimensional anomalies in the input file, which is a possibility in a complex input file, the three-dimensional output will reveal the resulting discrepancies.

The coolant pressure at the exit of the cooling channels is an important design parameter for regeneratively cooled rocket engines. This is due to the fact that quite often the coolant, such as liquid hydrogen, is being used to run a turbo pump. In other cases the exit pressure at the injector must be above a specified value. The heat transfer from the hot-gas, as well as the cooling channel geometry influences the coolant pressure. This new TDK-RTE model is capable of effectively predicting the coolant pressure at all locations along the axial direction. Figure 9 shows the predictions of static and stagnation pressure distributions for the SSME. The results show that the coolant stagnation pressure at the cooling channel exit is about 4300 psi, which is generally adequate for running a turbo pump.

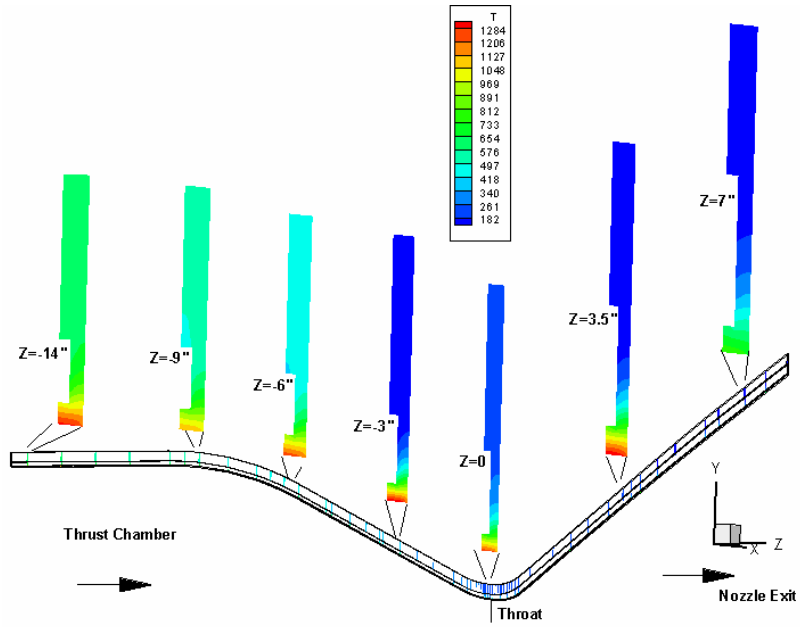

Figure 7. Three-dimensional Temperature Distribution for a SSME Cooling Channel

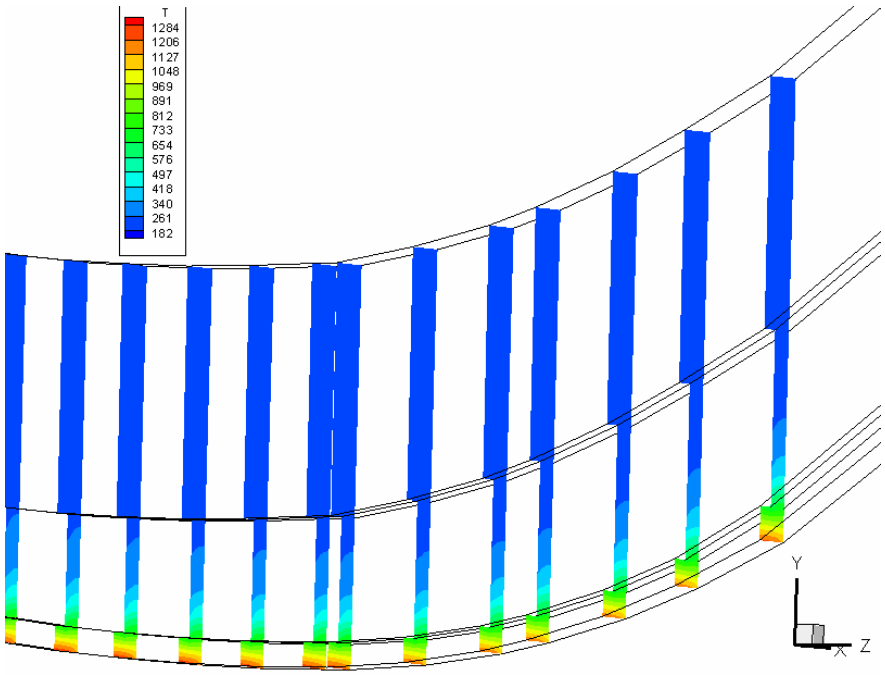

Figure 8. Zoomed-in Temperature Distribution at the SSME Throat

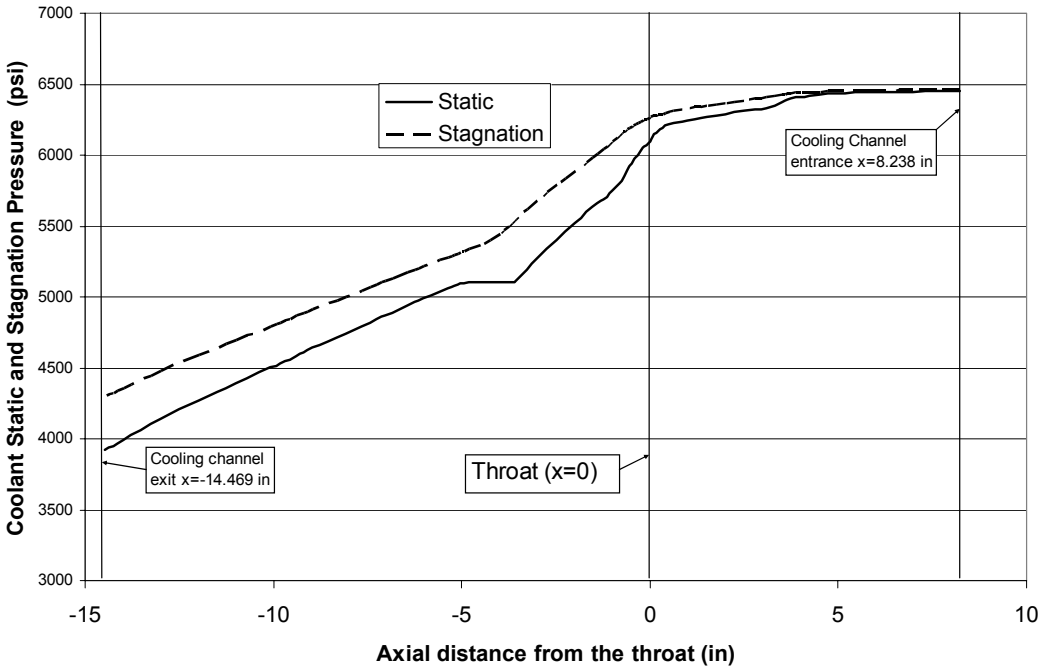

Figure 9. Predicted Static and Stagnation Pressure Distributions for the SSME (TDK-RTE Model)

B. Analysis of a RP1/LOX using LOX as the Coolant

A NASA Glenn LOX/RP1 rocket engine was analyzed to compare the results of the present TDK-RTE model with the experimental data. This engine was selected for analysis because experimental temperature data was available for LOX cooling in the throat region (Personal communications with H.G. Price and E.S. Roncase[4]). Specifications of this engine are as follows:

Chamber length:	11.5 in.
Chamber Diameter:	4.8 in.
Throat Diameter:	2.6 in.
Total length:	18.5 in.
Exit diameter:	6.25 in.
Coolant:	LOX
Chamber pressure:	variable 1000 to 2000 psia
O/F:	variable 1.8 to 2.98
Thrust	variable 9500 to 17000 lb

It should be noted that the cooling channel width is 0.5 inch at station (Z=-1.3 inch) and 0.4 inch at the throat. This increase in cooling channel width causes a slowdown of the coolant in the channel, which results in the reduction of the heat transfer coefficient (i.e., less cooling and larger wall temperature). Reducing cooling channel width would result in lower wall temperature at Z=-1.3 inch; however, it would significantly increase the pressure drop. The cooling channel width was reduced at the throat since there is not enough area for wider cooling channels.

The TDK-RTE model was used to predict the wall temperature distribution for the 2000 psia chamber pressure and O/F=2 case. The resulting wall temperature distributions for this engine are shown in Figure 10 and Figure 11. The maximum wall temperature of 1200 ºR occurs 1.3 inches upstream of the throat, as shown in the above figures. Figure 12 shows wall heat flux for all axial locations of this engine. The maximum wall flux is 45.48 BTU/sec-in^2, which is at 0.3 inches upstream of the throat (Z=-0.3 inch). The heat flux at the maximum temperature point is 33 BTU/sec-in^2 at 1.3 inch upstream of the throat (Z=-1.3 inch). The predicted wall temperature at the throat region based on the TDK-RTE model is 1015 ºR, while the measured temperature was 950 ºR (less than 7% difference). If a 0.0005-inch soot layer is added to the inner surface of the chamber and nozzle, then the predicted temperature at the surface of throat becomes 955 ºR (almost the same as the measured temperature). As stated in Huzel and Huang[7], the soot layer is significant in heat flux reduction for low chamber pressures (chamber pressure less than 1500 psi). The results based on the TDK-RTE model verify Huzel and Huang's conclusion. Generally, the soot layer can be neglected in the TDK-RTE results as long as the chamber pressure is more than 1500 psi.

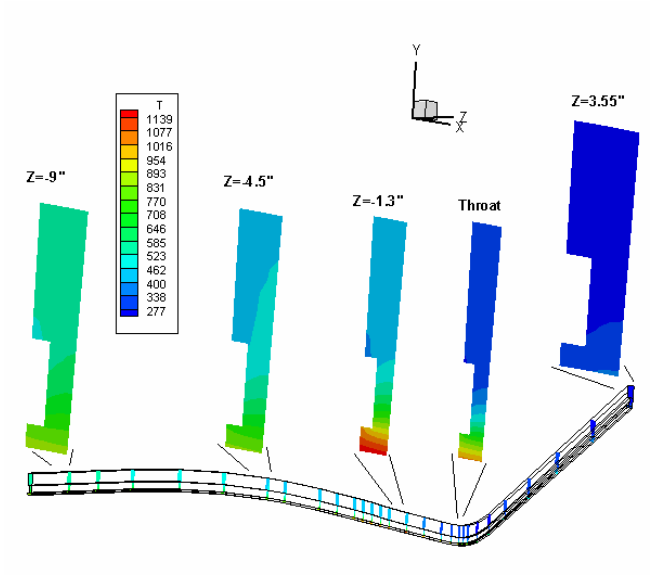

Figure 10. Wall Temperature Distribution for NASA's RP1-LOX Engine with LOX Cooling

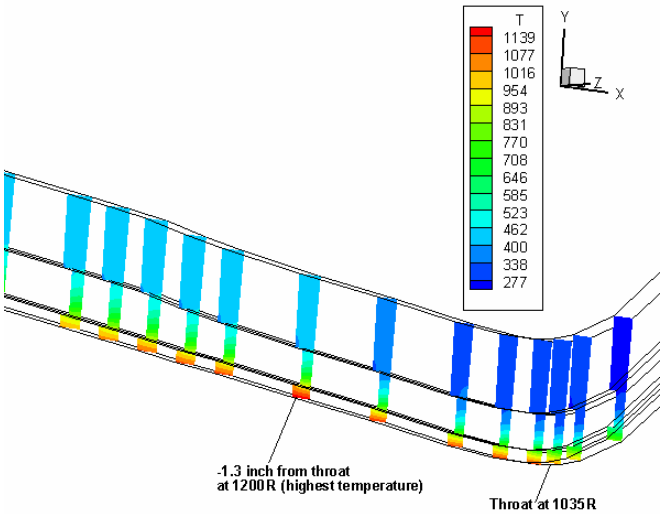

Figure 11. Throat Area Temperature Distribution Showing the Largest Temperatures

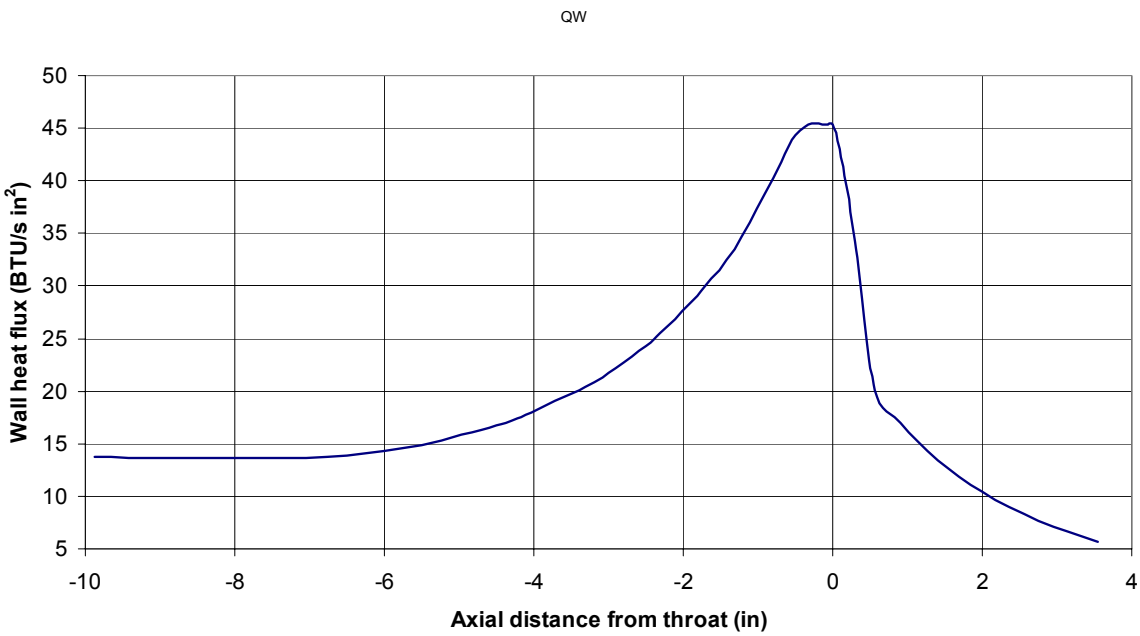

Figure 12. Wall Heat Flux vs. Axial Distance from the Throat for NASA's RP1-LOX Engine with LOX Cooling

Figure 13 shows the static and stagnation pressure along the cooling channels. As shown in this figure, the pressure drop is larger in the throat region than the thrust chamber and nozzle exit. This is due to the reduced cooling channel width at the throat. The results shown in Figure 13 can be used to evaluate the contribution various sections of the cooling channels add to the overall pressure drop in the cooling circuit. A large pressure drop in the cooling circuit is indicative of the requirement for large pumping power to move the coolant. The design of a viable cooling channel involves optimizing the wall temperatures (i.e., wall temperatures below the thermal limits of the material) and pumping power. In this configuration, for example, the maximum temperature of 1200 ºR is well below the design limit of the copper (1100 ºF, 1560 ºR) indicating a viable design.

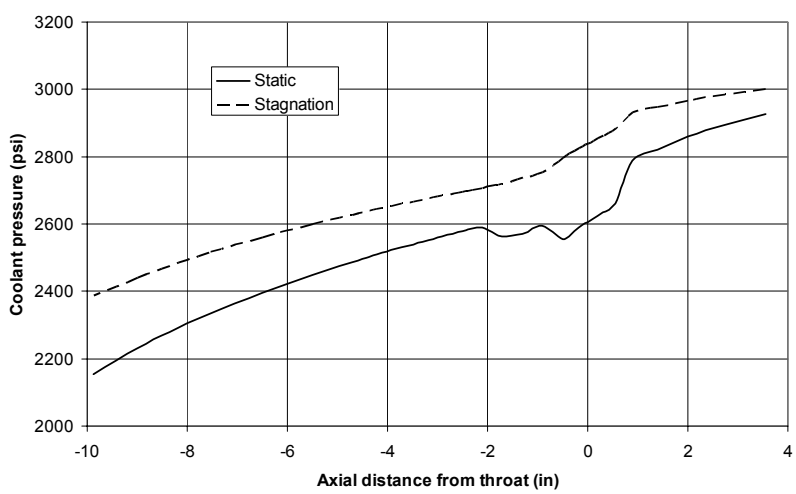

Figure 13. LOX Static and Stagnation Pressure Distribution in the Cooling Channels

Finally, Figure 14 shows coolant stagnation temperature at as a function of axial distance. The slope of this line is an indication of the amount of heat absorbed by the coolant along the axial length. The slope is mostly constant, except for a small portion upstream of the throat, where the heat flux is the largest. The reason for a smooth increase of the coolant temperature along the cooling channel is the overall heat flow, q"*A (product of heat flux and area) remains almost constant. This is caused by high heat flux where the area is the smallest (throat), and low heat flux where the area is large (chamber and nozzle exit).

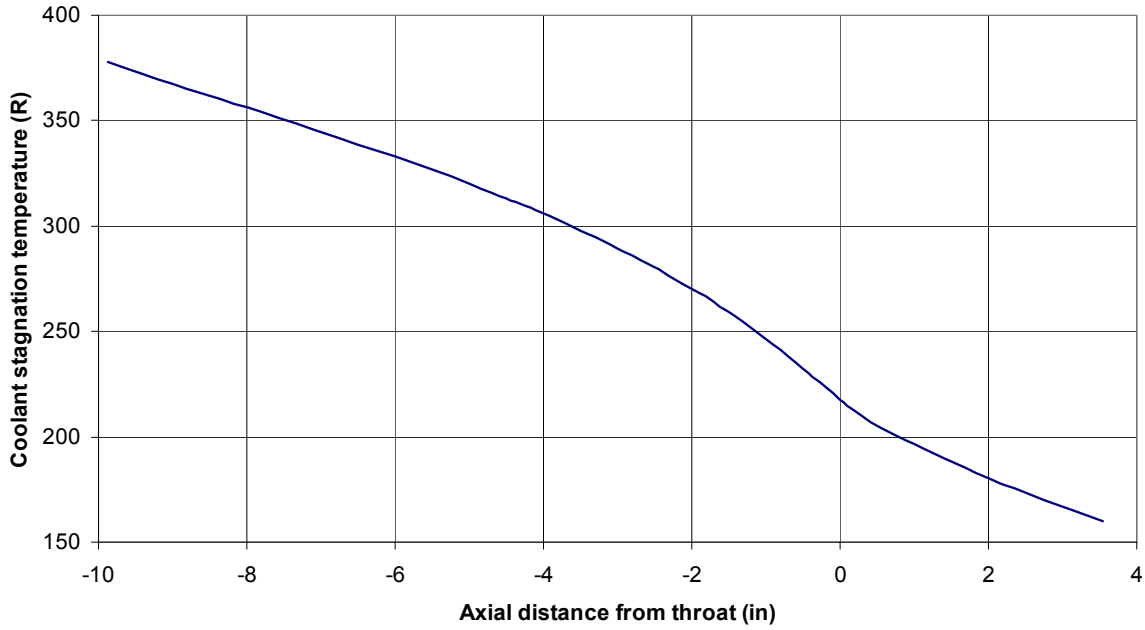

Figure 14. Coolant (LOX) Stagnation Temperature at Different Axial Locations

Although liquid oxygen cooling resulted in an acceptable cooling circuit design, any leakage of LOX into the chamber or nozzle can result in a catastrophic failure. Therefore, RP1 was investigated as an alternative cooling option. It is shown that this combined RTE-TDK model can be to come up with a viable RP1 cool engine.

IV. Concluding Remarks

A Stanton number lookup table is used to conjugate TDK and RTE for a comprehensive thermal analysis of regeneratively cooled rocket engines. The results obtained based on this model agree well with those of published results for the SSME and experimental data for a RP1/LOX engine with LOX cooling. This model only takes a few minutes to run making it an excellent tool for the design of the cooling circuit of a regeneratively cooled engine. The results of the wall temperature distributions of the SSME based on two different coolant-side correlations demonstrates that the calculated wall temperatures are highly sensitive to the selected coolant side correlation.

Although this paper presents the results for two engines, both with rectangular cooling channels, the program can be used to analyze engines with tubular cooling channels. This combined model can also be used to investigate cooling capabilities of hydrocarbon fuels.

V. Acknowledgement

This work is supported by Edwards Air Force SBIR Phase I contract F04611-03-M-3015.

VI. References

1. Dunn, S.S., Coats, D.E., and French, J.C., "TDK'02™ Two-Dimensional Kinetics (TDK) Nozzle Performance Computer Program", User's Manual, prepared by Software & Engineering Associates, Inc., Dec 2002.

2. Naraghi, M.H.N., "RTE - A Computer Code for Three-Dimensional Rocket Thermal Evaluation," User Manual, Tara Technologies, LLC, Yorktown Heights, NY 2002.

3. Wang, T.S., et al., "Hot-Gas-Side and Coolant-Side Heat Transfer in Liquid Rocket Engine Combustor", AIAA Journal of Thermophysics and Heat Transfer, 1994, Vol. 8, No. 3, pp 524-530.

4. Price, H.G. and Roncase, E.A., NASA Lewis Research Center, personal communication, 1986.

5. McCarthy, J.R., and Wolf, H., "Heat Transfer Characteristics of Gaseous Hydrogen and Helium," Rocketdyne Division of North American Aviation, Research Report RR-60-12, Canoga Park, CA, 1960.

6. Hendricks, R.C., Niino, M., Kumakawa, A., Yernshenko, V.M., Yaski, L.A., Majumdar, L.A., and Mukerjee, J., "Friction Factors and Heat Transfer Coefficients for Hydrogen Systems Operating at Supercritical Pressures", Proceeding of Beijing International Symposium on Hydrogen Systems, Beijing, China, May 7-11, 1985.

7. Huzel, D.K., and Huang, D.H., "Modern Engineering for Design of Liquid-Propellant Rocket Engines", Progress in Astronautics and Aeronautics, AIAA publication, Vol. 147, 1992.